Direct Synthesis and Reactivity of Unsupported (η^3-Oxaallyl)rhodium(I) Complexes

Greg A. Slough,*,† Randy Hayashi,‡ John R. Ashbaugh,† Sheri L. Shamblin,† and Amy M. Aukamp†

Departments of Chemistry, The College of Wooster, Wooster, Ohio 44691, and The University of Wisconsin at Madison, Madison, Wisconsin 53706

Received August 25, 1993®

Addition of 2 equiv of $K^+PhC(O)CH_2^-$ to $[(Ph_3P)_2RhCl]_2$ (1) gave the monomeric (η^3-oxaallyl)rhodium complex $(Ph_3P)_2Rh(\eta^3\text{-}CH_2C(O)Ph)$ (3). Reaction of 1 with $K^+t\text{-}BuC(O)CH_2^-$ produced a similar oxaallyl complex (6), which was characterized by spectroscopic methods and by X-ray crystallography. Both 3 and 6 showed dynamic NMR spectra which equilibrated the methylene protons at 25 °C. A general methodology for the preparation of (η^3-oxaallyl)rhodium complexes was developed by starting from $[(COD)RhCl]_2$ (7) and 4 equiv of phosphine. Complexes $(Et_3P)_2Rh(\eta^3\text{-}CH_2C(O)Ph)$ (8) and $(Et_3P)_2Rh((Z)\text{-}\eta^3\text{-}CH_3CHC(O)\text{-}t\text{-}Bu)$ (10) were prepared by this methodology. No fluxional behavior was observed with either 8 or 10. Oxaallyl 8 reacted rapidly with CO and *t*-BuNC to produce the η^1-oxygen-bound rhodium enolates *trans*-$(Et_3P)_2(CO)Rh(OC(Ph)CH_2)$ (12) and *trans*-$(Et_3P)_2$(t-BuNC)$Rh(OC(Ph)CH_2)$ (13). However, unlike complex 8, oxaallyl 6 added 2 equiv of *t*-BuNC, giving a trigonal-bipyramidal carbon-bound rhodium enolate complex (16). Notable differences in reactivity between rhodium oxaallyl and rhodium allyl complexes are explained in terms of enhanced stability of the η^1-oxygen-bound rhodium complex relative to the η^1-allyl complex.

Transition metal complexes containing the η^3-allyl ligand are among the most common and useful compounds in organometallic chemistry.[1] Stoichiometric and catalytic (η^3-allyl)palladium complexes are, perhaps, the reagents of choice for allylic transformations,[2] while unsymmetrical allyl complexes, such as $CpMo(NO)Cl(\eta^3\text{-allyl})$, are powerful reagents for asymmetric synthesis.[3] Despite these developments, little effort has been devoted to extend this work to the isoelectronic η^3-oxaallyl complexes. This is surprising, since the chemistry of η^3-oxaallyl complexes interfaces both the chemistry of η^3-allyl complexes and transition-metal enolate complexes.

Few examples of η^3-oxaallyl complexes are known. Shapley reported a dinuclear ruthenium complex with an η^3-oxaallyl ligand resulting from the reaction of a bridging ketene complex and CO.[4] Whimp characterized a mononuclear (η^3-oxaallyl)manganese complex which arose from the addition of an acetyl group to the vinyl group of the (2-vinylphenyl)diphenylphosphine ligand.[5] Both of these complexes supported the oxaallyl ligand by linking it to accompanying ancillary ligands. Bergman and Heathcock studied the photolysis of η^1-tungsten enolate complexes and found that a variety of unsupported (η^3-oxaallyl)-tungsten complexes can be produced by this methodology.[6] Each of these preparative methods require that coordinative unsaturation be generated in the presence of an η^1(C) enolate ligand. In this paper, we report an alternative synthesis of unsupported η^3-oxaallyl complexes through the direct addition of potassium enolates to (μ-dichloro)rhodium dimers.[7] The monomeric rhodium oxaallyl complex $(Ph_3P)_2Rh(\eta^3\text{-}OC(t\text{-}Bu)CH_2)$ was characterized by X-ray crystallography, providing unequivocal evidence for η^3-binding of the enolate ligand. We also detail the reactivity of (η^3-oxaallyl)rhodium complexes with CO and *tert*-butyl isocyanide.

Results

Preparation of (η^3-Oxaallyl)rhodium Complexes from Bis(μ-chloro)tetrakis(triphenylphosphine)-dirhodium. Addition of solid $PhC(O)CH_2^-K^+$ (2) to a suspension of $[(Ph_3P)_2RhCl]_2$ (1) in THF resulted in rapid formation of the soluble oxaallyl complex $(PPh_3)_2Rh(PhC(O)CH_2)$ (3). Extraction of the orange-yellow oxaallyl complex into ether, followed by filtration of the insoluble KCl and recrystallization, gave a 62% yield of yellow-orange microcrystals of 3. Exposure of 3 to air in the solid state led to complete decomposition of the crystals over 1 h, giving acetophenone and a mixture of rhodium products. Under inert conditions, however, a solution of 3 in C_6D_6 decomposed smoothly at 100 °C (3 half-lives measured, $k = 7.5 \times 10^{-4}$ min^{-1}, $t_{1/2} = 15.2$ h), giving acetophenone and a mixture of unidentified rhodium compounds. The triphenylphosphine region of the ^{1}H NMR was very complex, indicating that numerous phosphine-containing species were present.

† The College of Wooster.
‡ The University of Wisconsin at Madison.
® Abstract published in *Advance ACS Abstracts*, February 1, 1994.

(1) (a) Collman, J. P.; Hegedus, L. S.; Norton, J. R.; Finke, R. G. *Principles and Applications of Organotransition Metal Chemistry*; University Science Books: Mill Valley, CA, 1987; Chapter 19. (b) Elschenbroich, C.; Salzer, A. *Organometallics*; VCH: Weinheim, FRG, 1989; pp 280–289.

(2) (a) Trost, B. M. *Tetrahedron* **1977**, *33*, 2615. Trost, B. M. *Acc. Chem. Res.* **1980**, *13*, 385. (b) Heck, R. F. *Palladium Reagents in Organic Synthesis*; Academic Press: New York, 1985.

(3) (a) Faller, J. W.; John, J. A.; Mazzieri, M. R. *Tetrahedron Lett.* **1989**, *30*, 1769. (b) Faller, J. W.; Linebarrier, D. L. *J. Am. Chem. Soc.* **1989**, *111*, 1937.

(4) Holmgren, J. S.; Shapley, J. R.; Wilson, S. R.; Pennington, W. T. *J. Am. Chem. Soc.* **1986**, *108*, 508.

(5) (a) Bennett, M. A.; Robertson, G. B.; Watt, R.; Whimp, P. O. *J. Chem. Soc. D* **1971**, 752. (b) Robertson, G. B.; Whimp, P. O. *Inorg. Chem.* **1973**, *12*, 1740.

(6) Burkhardt, E. R.; Doney, J. J.; Bergman, R. G.; Heathcock, C. H. *J. Am. Chem. Soc.* **1987**, *109*, 2022.

(7) A personal communication from T. Tulip reporting the preparation of $(Et_3P)_2Rh(\eta^3\text{-}OC(Ph)CH_2)$ was cited in ref 6, but this work has never been published.

0276-7333/94/2313-0890$04.50/0

Scheme 1

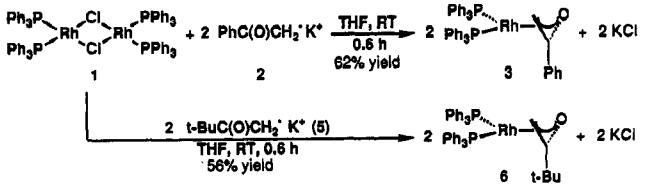

The ^1H NMR spectrum of **3**, conducted at 25 °C in C_6D_6, showed two converging signals centered at δ 3.48 that were integrated to two hydrogens. This signal was assigned to the methylene protons. The 0.8 ppm upfield shift of the $=CH_2$ resonance compared to that in the η^1-oxygen-bound rhodium enolate[8] is consistent with increased electron density at the α-carbon of the oxaallyl group. Both triphenylphosphine ligands showed different sets of proton resonances, indicating an unsymmetrical rhodium complex.

The $^{31}P\{^1H\}$ NMR established an unsymmetrical pseudo-square-planar geometry at the rhodium center. Two ABX signals appeared at δ 38.8 (J = 196.4, 35.5 Hz) and δ 53.9 (J = 225.6, 35.5 Hz). The phosphorus signal at δ 53.9 (trans to the α-carbon) followed the phosphorus chemical shift of the structurally similar (η^3-methallyl)-bis(triphenylphosphine)rhodium complex.[9] The phosphorus trans to the oxygen, however, shifted 15 ppm upfield, demonstrating that this phosphine ligand efficiently back-bonds with the rhodium and thereby removing electron density from the metal. The phosphorus signals of **3**, in toluene-d^8, remained unchanged over the temperature range of −45 to 53 °C. However, a broad signal at δ 60.2, which was integrated to approximately 3% of the oxaallyl signal, became evident below −15 °C.

The broad methylene signal in the ^1H NMR and the transient species at low temperature in the phosphorus spectrum suggested that an exchange process for the two methylene hydrogens occurred in complex **3**. Variable-temperature ^1H NMR studies provided evidence for this conclusion. At −62 °C, a toluene-d^8 solution of **3** (0.015 M) showed two signals at δ 3.67 and 3.48 (see Figure 1).[10] When the temperature was raised to −30 °C, the downfield signal at δ 3.52 split into a doublet (J_{P-H} = 10 Hz) while the signal at δ 3.37 remained a broad singlet. The large P–H coupling (10 Hz) followed the trend found in rhodium allyl complexes in which the anti hydrogens of the allyl show large P–H coupling.[11,12] At ~10 °C the methylene signals coalesced into a single broad resonance centered at δ 3.34.

Line-shape analysis of the proton signals in Figure 1 indicated that equilibration of the methylene hydrogens did not occur by a simple two-site exchange process. Rather, the signals in **3** remained well resolved until close to the coalescence temperature, at which point the signals moved together rapidly. Because the signal did not converge at the weighted average of the two methylene resonances, it suggested that an intermediate interceded in the equilibration. Moreover, the diastereotopic phosphorus signals did not equilibrate over a wide temperature range, indicating that a four-coordinate metallacycle such as **4** may be present (eq 1).[13] On the basis of a chemical

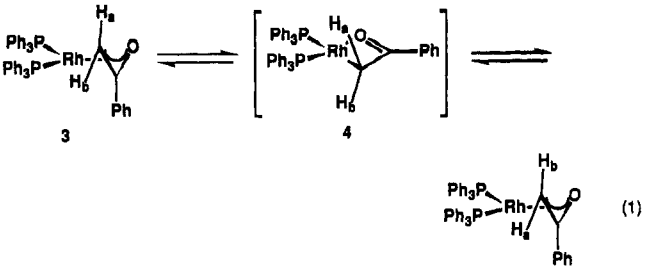

shift difference of 51 Hz between the two methylene resonances and the ^1H NMR coalescence temperature of 10 °C, a ΔG^* value of 13.9 kcal mol^{-1} was determined for the equilibration.[14]

In the carbon NMR of **3**, two resonances at δ 56.7 and 154.7 were important in confirming the bonding mode of the oxaallyl ligand. The methylene carbon signal at δ 56.7 showed a 24-Hz coupling with the ^{103}Rh nuclei. Initially, the resonance for the quaternary carbon was difficult to observe; therefore, **3** was prepared using $Ph^{13}C(O)CH_2^-K^+$.[15] A closely spaced doublet at δ 154.7 (J_{Rh-C} = 4.6 Hz) became the dominant feature of the spectrum. The multiplicity of the enhanced signal gave unequivocal evidence for bonding interaction between the rhodium and the central carbon of the acetophenone ligand.

A second rhodium oxaallyl complex was prepared using the same synthetic strategy. The potassium enolate of 3,3-dimethyl-2-butanone ($(CH_3)_3CCO)CH_2^-K^+$; **5**) combined smoothly with $[(Ph_3P)_2RhCl]_2$ in THF, giving a 56% yield of **6** as a yellow powder. Many of the spectral features of **6** paralleled those of **3**, although there were notable differences. For instance, the methylene protons in **6** appeared as two very broad resonances centered at δ 3.57 and 2.82. The distinct chemical shifts for the two methylene hydrogens indicated that the activation barrier for fluxional interconversion of the two protons was slightly higher for **6** than for **3**. Coalescence of the two methylene signals occurred at 35 °C, giving $\Delta G^{\ddagger}$ = 14.4 kcal mol^{-1} for the equilibration.

The phosphorus and carbon NMR spectroscopy of **6** was again indicative of η^3-ligand bonding. The phosphorus resonances at δ 55.2 (J = 222, 37 Hz) and δ 37.0 (J = 193, 37 Hz) demonstrated the square-planar geometry of **6**, while carbon resonances at 54.3 ppm (J_{Rh-C} = 24 Hz) and 175.0 ppm were assigned to the two carbons of the η^3-oxaallyl ligand. The 20 ppm downfield shift for the quaternary carbon was surprising, since the electron donation from the *tert*-butyl group, relative to the phenyl group of **3**, should shift the quaternary resonance upfield. Gated carbon NMR revealed a 153 Hz C–H coupling for the methylene carbon. This coupling value was similar to the C–H coupling in **3** (154 Hz), indicating that the methylene carbon retained substantial sp^2 hybrid character. Main-group enolates and η^1-transition-metal enolates have been classified as carbon-bound or oxygen-bound tautomers on the basis of the magnitude of the α-carbon C–H coupling.[16] Coupling constants >150 Hz have been interpreted as oxygen-bound enolates with the α-carbon

(8) Slough, G. A.; Bergman, R. G.; Heathcock, C. H. *J. Am. Chem. Soc.* **1989**, *111*, 938.
(9) Reilly, C. A.; Thyret, H. *J. Am. Chem. Soc.* **1967**, *89*, 5144.
(10) Resolution of the proton signals decreased below −40 °C presumably due to limited solubility at lower temperatures.
(11) Sivak, A. J.; Muetterties, E. L. *J. Am. Chem. Soc.* **1979**, *101*, 4878.
(12) Fryzuk, M. D. *Inorg. Chem.* **1982**, *21*, 2134.
(13) A three-coordinate carbon-bound enolate is an unlikely intermediate, since the phosphines would equilibrate on the same time scale as the methylene hydrogens.
(14) Johnson, C. S. *Adv. Magn. Reson.* **1965**, *1*, 33.
(15) [^{13}C]benzoic acid was prepared from PhLi and $^{13}CO_2$, and then the method of Tegner was followed for the preparation of [^{13}CO]-acetophenone. Tegner, C. *Acta Chem. Scand.* **1952**, *6*, 782.

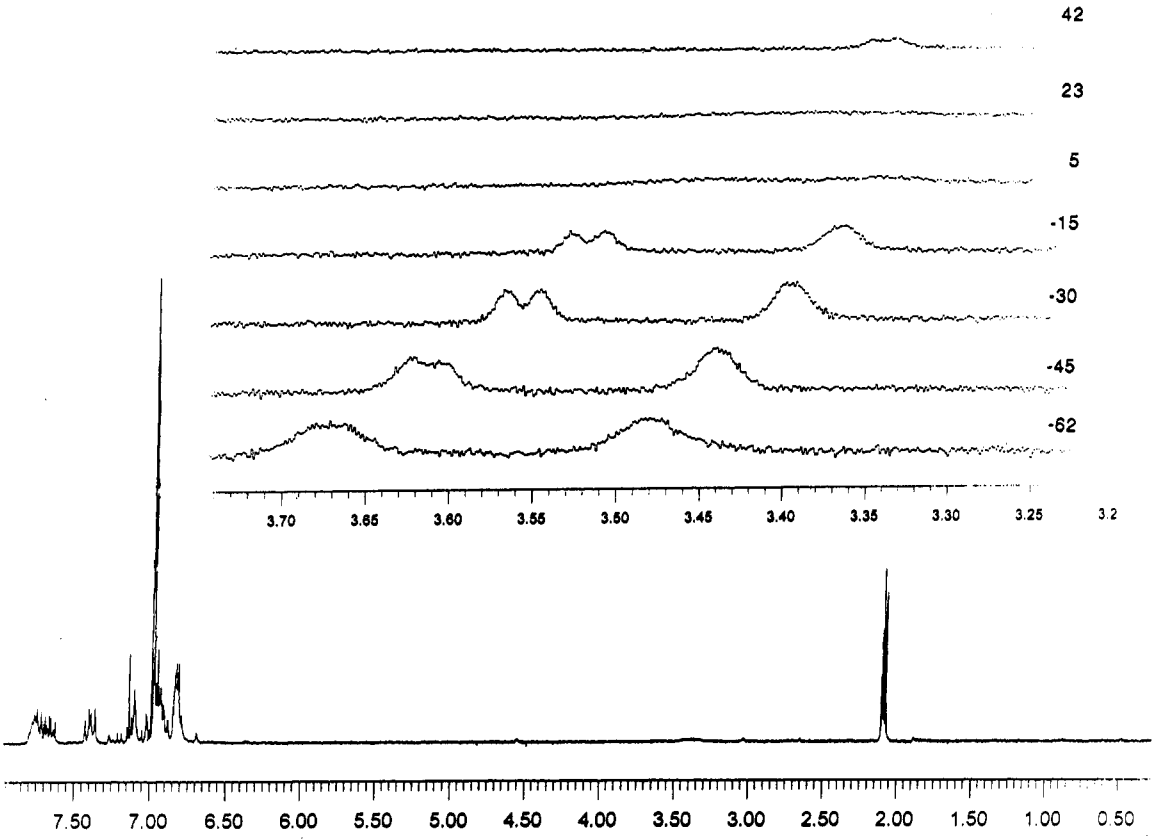

Figure 1. Variable temperature ^1H NMR (270 MHz) of **3** in toluene-d_8 (temperature reported in kelvin).

Table 1. Spectral Data for Bis(phosphine)rhodium η^3-Oxaallyl and η^3-Allyl Complexes

			chem shift, δ (J_{P-H} in Hz)				
complex	solvent	temp (°C)	H_{1syn}	H_{1anti}	C_1	C_2	$J_{C(1)-H}$ (Hz)
3	C_6D_6	24	3.48 (broad, 2H)		55.7	154.7	154
	$C_6D_5CD_3$	−30	3.39	3.52 (6.0)			
6	C_6D_6	24	2.82	3.57	54.3	175.0	153
	$C_6D_5CD_3$	−25	2.77	3.63 (5.0)			
8	C_6D_6	24	3.27 (4.9)	3.65 (1.0)	48.2	151.9	154
10	C_6D_6	24	3.64 (3.0)		56.4	161.4	152
$(Ph_3P)_2RH(\eta^3$-allyl)	C_6D_6	24	3.08	2.51 (4.0)	58.9	107.1	

being sp^2 hybridized. The carbon-bound enolates of mercury[17] and tungsten[6] show smaller C–H coupling, typically around 140 Hz, and the hybridization of the α-carbon is commonly described as sp^3.

The structure of **6** was confirmed by single crystal X-ray analysis (see Figure 2). X-ray quality crystals of **6** grew from a concentrated C_6D_6 solution as small orange blocks. The $P2_1/c$ space group of the unit cell contained four molecules of **6** and four molecules of C_6D_6. Structurally the rhodium atom is surrounded by the η^3-oxaallyl ligand and the two phosphine ligands in a pseudo-square-planar geometry. The rhodium, two phosphorus atoms, and oxygen atom are coplanar. The fourth coordination site is occupied by the C(1)–C(2) bond. Atoms C(1) and C(2) are displaced equally above and below the square plane by 0.4 Å. Ligation of the unsymmetrical oxaallyl group causes a distinct trans ligand effect. The P(2)–Rh bond is 2.275 Å in length, matching closely the phosphorus–rhodium bond length in the $(Ph_3P)_2Rh(\eta^3$-$CH_2C(CH_3)$-$CH_2)$ complex.[18] The P(1)–Rh distance, on the other hand, is ~0.1 Å shorter than the P(2)–Rh bond. Electron donation by the oxygen atom to the rhodium accentuates π back bonding by the P(1) phosphine ligand, which strengthens the P(1)–Rh interaction.

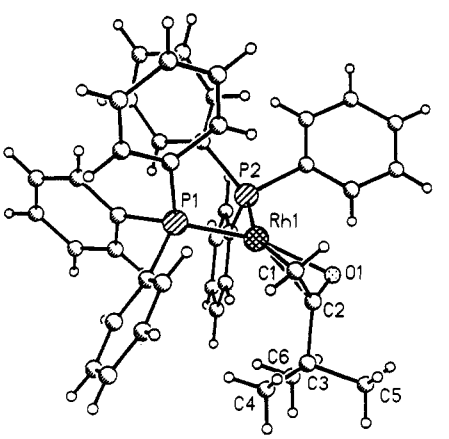

Figure 2. X-ray crystal structure of $(Ph_3P)_2Rh(\eta^3$-$OC(t$-Bu)-$CH_2)$ (**6**) (50% thermal ellipsoids shown).

The dihedral angle between the plane of the η^3-oxaallyl group and the plane of the rhodium atom in **6** is 118.9°. This angle is somewhat larger than the angle found in symmetric (π-allyl)rhodium complexes. For example, the bis(dicyclohexylphosphine)rhodium methallyl complex

(16) Hansen, M. M.; Bartlett, P. A.; Heathcock, C. H. *Organometallics* 1987, *6*, 2069. See references therein.
(17) Meyer, R.; Gorrichon, L.; Maroni, P. J. *J. Organomet. Chem.* 1977, *129*, C7.
(18) Murray, B. D.; Power, P. P. *Organometallics* 1984, *3*, 1199.

Table 2. Selected Bond Lengths (Å) and Angles (deg) for $(Ph_3P)_2Rh(\eta^3\text{-}OC(t\text{-}Bu)CH_2)$ (6)

Rh–C(1)	2.163(8)	Rh–P(1)	2.189(2)
Rh–C(2)	2.208(7)	Rh–P(2)	2.275(2)
Rh–O(1)	2.131(5)		
C(1)-C(2)-O(1)	116.5(7)	P(1)-Rh-P(2)	98.8(1)
C(1)-Rh-O(1)	64.6(3)	C(1)-C(2)-C(3)	124.8(7)

Scheme 2

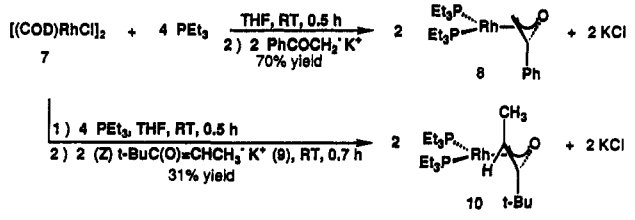

shows a dihedral angle of 107.6°.[19] However, the dihedral angle in **6** lies within the range of 110–125° found in most four-coordinate palladium–π-allyl compounds.[19] The wider interplane angle in **6** presumably better accommodates the bulky *tert*-butyl group and enhances bonding with the terminal atoms of the oxaallyl ligand.[20] A larger dihedral angle in **6** may also account for the downfield shift of the C(2) carbon resonance. As C(2) assumes a wider dihedral angle relative to the P–Rh–P plane, this carbon becomes more carbonyl-like and the carbon resonance shifts to lower field. This suggests that the carbon resonance of C(2), rather than the C–H coupling constant, is an important criterion of oxaallyl structure.

Preparation of η^3-Oxaallyl Complexes from [(COD)RhCl]$_2$. In an attempt to find a versatile rhodium precursor for oxaallyl complexes, $[(COD)RhCl]_2$ (**7**) was examined. Addition of 4 equiv of PEt_3 to a suspension of $[(COD)RhCl]_2$ in THF resulted in rapid dissolution of the organometallic reagent. Solid $PhC(O)CH_2^-K^+$ reacted smoothly with the *in situ* prepared (μ-dichloro)rhodium dimer, giving a 70% yield of oxaallyl **8** after recrystallization from pentane. Characterization of **8** followed the spectral features of **3** and **6**. A notable exception was the phosphorus–proton coupling observed in the methylene protons. The anti proton at C(1) appeared as a doublet (J = 4.9 Hz) at δ 3.27, while the syn proton resonated at δ 3.65, appearing as a closely spaced doublet (J < 1.0 Hz). The relative chemical shifts and coupling constants for these proton signals were similar to those in (η^3-allyl)rhodium complexes.[10] Because discrete methylene resonances were observed at room temperature, complex **8** is stereochemically rigid compared to **3** and **6**. Not surprisingly, this indicates that electron-donating phosphine ligands strengthen π-bonding between the oxaallyl ligand and the rhodium center. Further evidence for the enhanced stability of **8** came from thermal decomposition studies. The decomposition of **8** in C_6D_6 at 100 °C displayed unimolecular kinetics through 3 half-lives. The $t_{1/2}$ value for the decay was 62 h ($k = 1.83 \times 10^{-4}$ min^{-1}), approximately 4 times the half-life of **3** under identical conditions.

The final preparation of an oxaallyl complex tested the geometric integrity of the oxaallyl ligand. When added to the *in situ* (μ-dichloro)rhodium dimer, the (*Z*)-enolate of 4,4-dimethyl 3-pentanone, (Z)-t-$BuC(O)=CHCH_3^-K^+$[20] (**9**), gave a single oxaallyl complex, **10**. Complex **10** recrystallized from pentane as golden yellow plates in 31% yield. The *Z* geometry of the oxaallyl group was assigned on the basis of the coupling pattern of the methine proton signal at δ 3.64. The methine signal appeared as a doublet of quartets (J_{H-H} = 6.0 Hz, J_{Rh-H} = 3.0 Hz). The relatively small rhodium–proton coupling is consistent with an oxaallyl geometry which positions the hydrogen at C(2) syn to the *tert*-butyl group. The methine proton signal remained unchanged over 3 days in C_6D_6 solution, indicating that β-hydrogen elimination and geometric isomerization are not important processes. This is significant, since putative palladium η^3-oxaallyl complexes containing β-hydrogens eliminate readily, forming α,β-unsaturated carbonyl compounds.[21]

Scheme 3

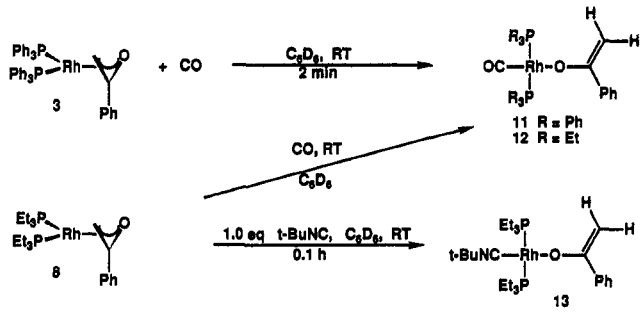

Reaction of Oxaallyl Complexes with CO and *t*-BuNC. Rhodium oxaallyl complexes **3** and **8** reacted very rapidly with CO, producing the trans η^1-oxygen-bound enolates **11** and **12** (see Scheme 3).[9] Both reactions were complete within 2 min at room temperature in C_6D_6 and were characterized by a color change from orange to yellow. The methylene protons for enolate **11** appeared as a broad singlet at δ 4.38. The aromatic phosphine signals simplified into two broad singlets at δ 7.00 and 7.86. Each proton resonance matched literature values for this complex.[9] Furthermore, the infrared spectrum of **11** showed a strong metal carbonyl band at 1965 cm^{-1} consistent with a trans-square-planar rhodium complex. Complex **12** displayed similar spectral features. The methylene protons appeared as two sharp singlets at δ 4.45 and 4.70. The diastereotopic triethylphosphine signals in **8** collapsed to a single set of resonances upon addition of CO, providing strong evidence for the trans-rhodium geometry of **12**.

Oxaallyl **8** also reacted smoothly with *tert*-butylisocyanide, giving complex **13**. This result was important, since it demonstrated that the formal coordinative unsaturation of oxaallyl complexes could be utilized to prepare a variety of η^1 rhodium enolate complexes. Proton and carbon NMR studies established the oxygen-bound tautomeric structure. The methylene protons of the enolate ligand appeared downfield at δ 4.69 as a broad singlet. In the carbon NMR spectrum, the quaternary carbon bearing the oxygen appeared at δ 167.6. This chemical shift was quite similar to that for other oxygen-bound rhodium enolates. For example, the central enolate carbon of *trans*-$(PMe_3)_2(CO)Rh$–$OC(Ph)CH_2$ appeared at δ 166.8.[9] A second diagnostic signal in the ^{13}C NMR corresponded to the complexed isocyanide. The isocyanide carbon resonated downfield relative to the free isocyanide and appeared as a triplet at δ 126.3. Two equivalent

(19) Vrieze, K. In *Dynamic Nuclear Magnetic Resonance Spectroscopy*; Jackman, L. M., Ed.; Academic: New York, 1975; Chapter 11.
(20) Heathcock, C. H., Buse, C. T.; Kleschick, W. A.; Pirrung, M. C.; Sohn, J. E.; Lampe, J. *J. Org. Chem.* **1980**, *45*, 1066.
(21) (a) Ito, Y.; Hirao, T.; Saegusa, T. *J. Org. Chem.* **1978**, *43*, 1011. (b) Ito, Y.; Aoyama, H.; Mochizuki, A.; Saegusa, T. *J. Am. Chem. Soc.* **1979**, *101*, 494.

Scheme 4

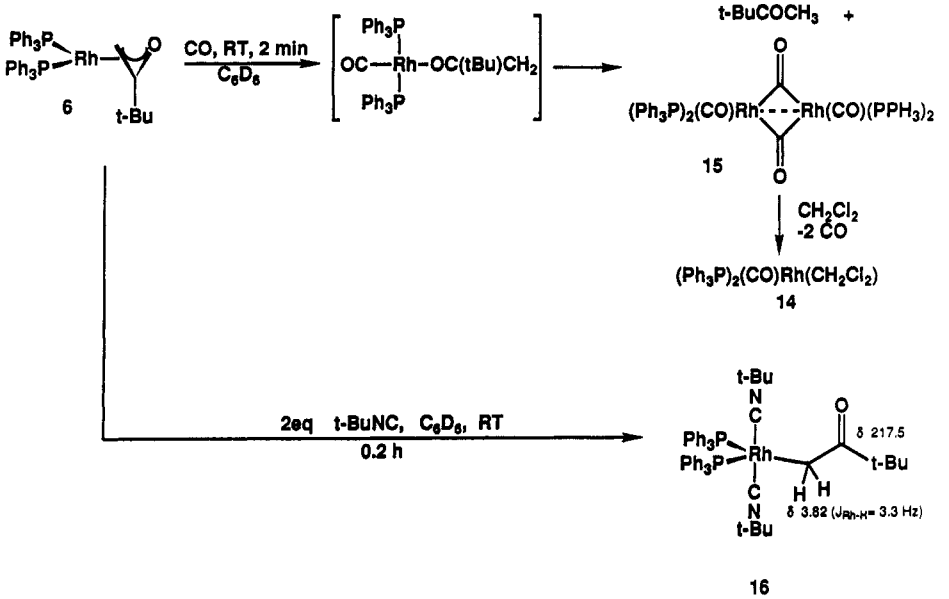

phosphorus atoms on the rhodium split the isocyanide signal, giving rise to the higher multiplicity.

Oxaallyl 6 reacted differently with both carbon monoxide and *tert*-butylisocyanide, yielding unexpected products. In each case, the unique chemistry was a manifestation of the incipient η^1-enolate rather than the oxaallyl complex. Bubbling CO gas through a C_6D_6 solution of 6 for 2 min resulted in a bright yellow precipitate. NMR analysis of the organic solution showed clean formation of pinacolone. No evidence for a rhodium enolate was found. Dissolution of the yellow solid in CH_2Cl_2 gave an orange-red solution which displayed two strong bands at 1991 and 1747 cm^{-1} and a broad weak signal at 1767 cm^{-1} in the infrared spectrum. These signals closely matched the metal carbonyl bands observed for the CH_2Cl_2-solvated mononuclear complex $(Ph_3P)_2(CO)Rh(CH_2Cl_2)$ (14).[22] Wilkinson found that the bright yellow $(Ph_3P)_2(CO)Rh(\mu\text{-}CO)_2Rh(CO)(Ph_3P)_2$ complex, 15, reacted rapidly in CH_2Cl_2, forming the solvated mononuclear complex. Disproportionation of the η^1-enolate in the presence of CO generates 15 and the methyl ketone radical, which after hydrogen abstraction produces the methyl ketone. Features of the η^1-pinacolone enolate intermediate which destablize it with respect to the η^1-acetophenone enolate are not known. However, exchange reactions between rhodium enolates and methyl ketones showed that electron-withdrawing substituents on the enolate ligand increased the thermodynamic stability of the enolate complex.[9]

Oxaallyl 6 also showed unique reactivity with *tert*-butylisocyanide. Addition of 1 equiv of *tert*-butylisocyanide to freshly prepared 6 produced a 1:1 mixture of starting oxaallyl and the new rhodium complex 16. Addition of a second equivalent of isocyanide gave 16 in >90% purity (see Scheme 4). Compound 16 could not be purified further from the reaction mixture. Upon concentration of the reaction mixture, an oily residue resulted which darkened over 0.2 h to orange-brown. Redissolving the concentrated sample in C_6D_6 gave new resonances in the NMR which accounted for ~30% of the mixture. One of the major byproducts was pinacolone. Before concentration, however, clean proton and carbon NMR spectra of 16 could be obtained. Two different *tert*-butyl resonances, which were integrated in a 2:1 ratio, appeared at δ 0.90 and 1.75, respectively, in the ^1H NMR. The equivalence of two *tert*-butyl resonances indicated that a symmetric 5-coordinate complex formed during isocyanide addition. A single set of triphenylphosphine resonances at δ 7.06 and 7.63 supported this conclusion. Moreover, the methylene protons of the pinacolone ligand appeared at δ 3.31 as a doublet (J_{Rh-H} = 3.3 Hz). The chemical shift of this signal was upfield ~1 ppm compared to the signal for oxygen-bound rhodium enolates, and the small coupling strongly suggested a η^1-carbon-bound structure. Carbon NMR spectroscopy showed a resonance at δ 217.5 which corresponded to the carbonyl carbon of the ketone ligand, adding further confirmation for the carbon-bound structure.

The geometry at the rhodium center could not be unambiguously determined, although infrared data provided evidence for a symmetric trigonal-bipyramidal geometry. A strong isocyanide stretch was found in the infrared spectrum at 2110 cm^{-1}. A smaller band at 2074 cm^{-1} (relative integrated intensity 8%) was present in all samples; however, the intensity of this lower energy signal depended upon the purity of the sample. A moderate band at 1612 cm^{-1} was also observed which was assigned to the ketone carbonyl stretch. The single band pattern for the isocyanide ligands excluded a square pyramidal structure, since symmetric and asymmetric stetches should be observed. Similar considerations excluded a trigonal-bipyramidal structure with the isocyanides in the equatorial plane. With all of the spectral data taken together, a trigonal-bipyramidal complex with the isocyanide ligands in the axial position and the 2-oxoalkyl ligand in the equatorial plane has been tentatively assigned as the structure of 16.

Formation of 16 presumably proceeds initially through a four-coordinate square-planar intermediate (A). Addition of the second isocyanide ligand to the axial position of the square-planar complex would generate an 18 e^- square-pyramidal complex with one isocyanide in the apical position and one in the basal plane (B). Twisting the isocyanide out of the basal plane and into an axial

(22) Evans, D.; Yagupshy, G.; Wilkinson, G. *J. Chem. Soc. A* 1968, 2660.

Scheme 5

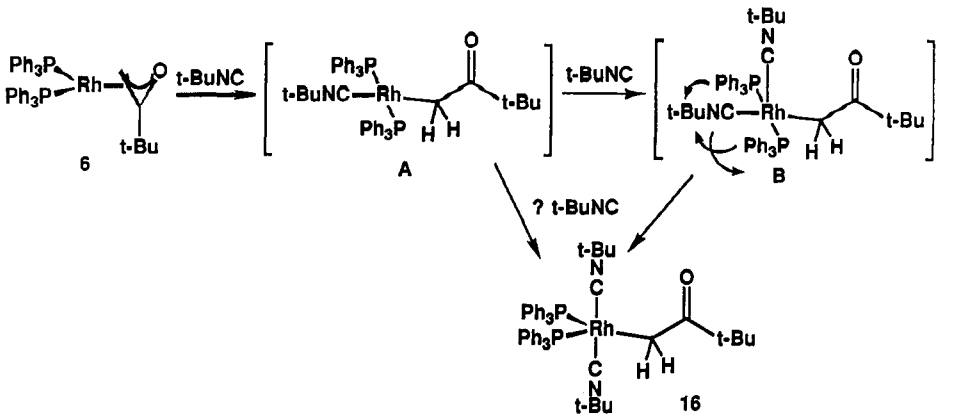

position would allow the bulky triphenylphosphine ligands to assume more spacious coordination sites in the equatorial plane of 16. The experimental evidence, however, cannot rule out direct conversion of the square-planar intermediate to the trigonal-bipyramidal product.

Acid–Base Properties of (η^3-Oxaallyl)rhodium Complexes. Treatment of 6 with acetophenone (1.1 equiv) in benzene resulted in slow exchange of the η^3-oxaallyl ligand over 43 h at 25 °C (eq 2). K_{eq} = 1.2 was determined for

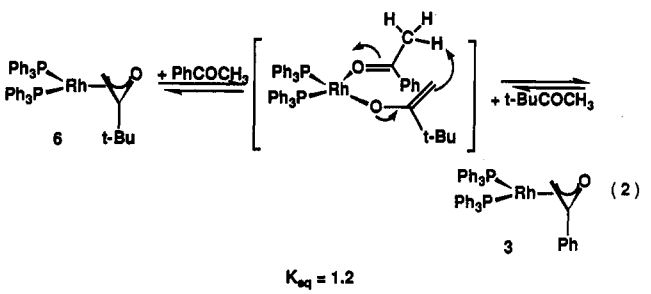

this exchange (95% mass balance). The small equilibrium constant suggested that 6 and 3 are quite similar energetically and that there is only a modest relief of steric strain by removing the *tert*-butyl group from the oxaallyl complex.

Electron-withdrawing groups on the oxaallyl ligand, however, had a substantial effect on the stability of the oxaally complex. For example, addition of *p*-nitroacetophenone (1.0 equiv) to a benzene solution of 8 gave a mixture of 8 and the new complex 17 in a 1.0:3.0 ratio after 48 h at 25 °C. Progress of the oxaallyl exchange was monitored by integration of the new singlet at δ 2.06 (acetophenone) and the methylene signals at δ 3.22 (a doublet (J_{P-H} = 5Hz)) and δ 3.42. The direction and extent of oxaallyl ligand exchange in this experiment followed thermodynamic acidity trends.[23] The more acidic ketone presumably protonated the basic oxaallyl ligand, causing oxaallyl ligand exchange. This trend also applies to ketones with high thermodynamic acidity, such as dibenzoylmethane. Addition of solid dibenzoylmethane (1.0 equiv) to a C_6D_6 solution of 3 gave complete exchange to complex 19 in less than 5 min. A single resonance at δ 56.75 (J_{Rh-P} = 196.4 Hz) was observed in the $^{31}P\{^1H\}$ NMR spectrum.

Two aspects of the oxaallyl ligand exchange are surprising. First, the oxaallyl ligand appears to be relatively

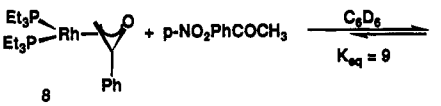

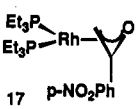

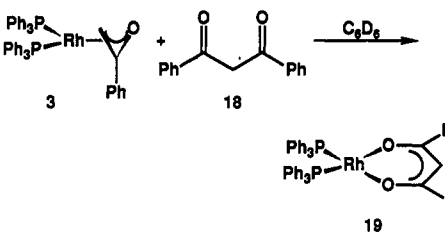

basic. A significant amount of electron density must be delocalized over the entire oxaallyl complex to achieve bonding. A substantial trans-ligand effect on the Rh–P bonds was noted in the crystal structure of 6, suggesting that electron density is distributed toward the phosphine ligands and away from the oxaallyl ligand. This distribution would decrease the basicity of the oxaallyl group. It is possible, however, that the basicity of the oxaallyl ligand is manifest mainly in the η^1-enolate tautomer. The open coordination site of the η^1-enolate tautomer could complex added methyl ketone, producing an intermediate capable of intramolecular proton exchange (eq 2). The second significant feature of oxaallyl ligand exchange is that nonpolar solvents function well as the reaction media. This contrasts with four-coordinate oxygen-bound rhodium enolates, which require polar solvents such as DMSO to facilitate exchange.[9] Again, a nonpolar, intramolecular transition state is a reasonable candidate for the exchange mechanism.

Discussion

Stable rhodium(I) oxaallyl complexes can be prepared directly from well- characterized dimeric rhodium complexes and potassium enolates. The oxaallyl group occupies two coordination sites at the metal center and acts as a four-electron-donor ligand. Structurally, η^3-oxaallyl complexes are very similar to the more familar (η^3-allyl)-rhodium complexes. Spectral evidence, such as rhodium–carbon splitting in the ^{13}C NMR and a distinctive ABX pattern in the ^{31}P NMR, shows definitively that all three atoms of the oxaallyl chain interact with the rhodium center.

(23) (a) Bordwell, F. G.; Bares, J. E.; McCollum, G. J.; Van Der Puy, M.; Mattews, W. S. *J. Org. Chem.* **1977**, *42*, 321. (b) Guthrie, J. P. *Can. J. Chem.* **1979**, *57*, 1177.

The chemistry of rhodium oxaallyl complexes, however, is fundamentally different from that of the isoelectronic rhodium allyl complexes. Oxaallyl complexes substituted with aromatic phosphine ligands are fluxional materials. This process rapidly equilibrates the syn and anti hydrogens of the oxaallyl group. In contrast, fluxional behavior in four-coordinate rhodium allyl complexes is unknown. Examples of dynamic processes in five- and six-coordinate rhodium(I) and rhodium(III) allyl complexes have been reported, however. Nixon observed temperature-dependent ^1H NMR and ^9F NMR spectra for $(PF_3)_3Rh(\eta^3\text{-}CH_2CHCH_2)$ and proposed both an η^3–η^1–η^3 and a phosphine dissociation mechanism for the fluxionality.[24] Green suggested similar intermolecular and intramolecular fluxional characteristics for (η^3-allyl)tris(trimethylphosphite)-rhodium.[25] Volger and Vrieze studied the syn–anti hydrogen exchange in the pseudo-six-coordinate $L_2Cl_2Rh(2\text{-}CH_3.\eta^3\text{-}CH_2CCH_2)$ complex and found the process to be consistent with an intramolecular η^3–η^1–η^3 mechanism.[26] The latter paper contended that electron-donating ligands facilitated η^3–η^1–η^3 equilibrations. This contention is in direct contrast to the situation with rhodium oxaallyls. Complexes **8** and **10** contain the potent electron-donating ligand PEt_3, but neither complex shows evidence of fluxional behavior even at elevated temperatures.

The dichotomy between rhodium oxaallyl and rhodium allyl complexes is most sharply apparent in their reactivity with Lewis bases. Addition of Lewis bases such as CO and *t*-BuNC to rhodium oxaallyl complexes rapidly yields four-coordinate η^1-rhodium enolates. Complex **6** added multiple isocyanides, yielding the unusual five-coordinate carbon-bound enolate complex. Rhodium allyl complexes, on the other hand, add dative ligands, but the η^3-allyl ligand is maintained. For example, $(Ph_3P)_2Rh(\eta^3\text{-}CH_3CH_2CHCH_2)$ adds CO at room temperature, leading to the unstable $(Ph_3P)_2(CO)Rh(\eta^3\text{-}CH_3CH_2CHCH_2)$ complex.[27] Independent synthesis of the CO adduct by Wilkinson confirmed the identity of the unstable complex.[28] The parent allyl complex $(Ph_3P)_2Rh(CH_2CHCH_2)$ reacts in a similar fashion with PF_3 to produce the isolable five-coordinate π-allyl complex $(Ph_3P)_2(PF_3)Rh(\eta^3\text{-}CH_2CHCH_2)$.[29] Ligand substitution also occurs with η^3-allyl complexes, leaving the η^3-allyl unit intact. For instance, carbon monoxide is extruded from $(CO)_2Rh(\eta^3\text{-}CH_2CHCH_2)$ by excess $P(OCH_3)$, giving the tris(trimethylphosphite) complex $(P(OCH_3))_3Rh(CH_2CHCH_2)$.

Addition and/or substitution reactions of rhodium oxaallyl and allyl complexes presumably occur by similar mechanistic pathways. Addition of the Lewis base to the 16 e$^-$ oxaallyl or allyl complex forms an initial 18 e$^-$ intermediate which either reorganizes to a discrete 18 e$^-$ complex or reverts to a four-coordinate, 16 e$^-$, square-planar complex with an η^1-ligand. Oxaallyls prefer the latter pathway, since a potent back-bonding ligand can be positioned trans to the η^1-enolate oxygen. This arrangement of donor–acceptor ligands stabilizes the rhodium–oxygen bond. Conversely, η^1-allyl complexes, being less electron donating, do not benefit from a similar trans-ligand effect and instead reorganize to an η^3-bound trigonal-bipyramidal complex.

In summary, monomeric η^3-rhodium oxaallyls are a distinct class of organometallic reagents. The oxygen atom in these complexes exerts fundamental influence on their structure and reactivity. The flexible bonding modes of the oxaallyl ligand, and the high electron density at rhodium open new possibilities for reactivity and catalysis with these complexes.

Experimental Section

General Considerations. All manipulations of air-sensitive materials were performed under nitrogen by vacuum-line techniques or in a Vacuum Atmospheres drybox equipped with an inert-gas purifier. Air-sensitive compounds were exposed to diethyl ether, tetrahydrofuran (THF), pentane, hexane, benzene, or benzene-d_6 (C_6D_6), which were dried over sodium and benzophenone immediately before use. Acetophenone (Aldrich), pinacolone (Aldrich), *p*-nitroacetophenone (Aldrich) dibenzoylmethane (Aldrich), were distilled or recrystallized prior to use. Triethylphosphine was stirred over sodium metal for 48 h prior to distillation under vacuum. Ethyl *tert*-butyl ketone,[29] $[(PPh_3)_2RhCl]_2$,[30] and $[(COD)RhCl]_2$[31] were prepared by literature methods.

^1H NMR spectra were acquired on Bruker WP200, WP270, and AM500 spectrometers. Gated and broad-band-decoupled ^{13}C NMR spectra were obtained on a Bruker WP270 (69.9 MHz), an AM400 (100.6 MHz), or an AM500 (126 MHz) instrument. Proton-decoupled $^{31}P\{^1H\}$ NMR spectra were obtained on a Bruker WP270 (109.4 MHz) or a BVX300 (121.5 MHz) spectrometer. Unless indicated otherwise, all NMR spectra were acquired at 25 °C. The chemical shifts were recorded relative to the residual benzene signal in benzene-d_6 (δ 7.16) in the ^1H NMR spectra and relative to the central carbon resonance of benzene (δ 128.0) in the carbon spectra. All ^{31}P NMR resonances were measured relative to 85% H_3PO_4. Infrared spectra were measured on a Mattson Polaris (FT) spectrometer. Mass spectra were determined on a KRATOS MS-80 instrument, and elemental analyses were performed by Galbraith Laboratories, Inc. (Knoxville, TN).

Preparation of (η^3-1-Phenyl-1-oxoethenyl)bis(triphenylphosphine)rhodium (3). In a glovebox, an oven-dried 25-mL round-bottom flask was charged with tetrakis(triphenylphosphine)dirhodium dichloride (**1**; 200 mg, 0.15 mmol). The solid was suspended in THF (10 mL), and solid potassium 1-phenyl-1-oxidoethene (**2**; 47 mg, 0.30 mmol) was added in one portion. On a vacuum line the suspension was stirred vigorously for 36 min. After concentration *in vacuo* the orange-yellow residue was triturated in hexane (15 mL) at −30 °C and then filtered through a reversible frit, yielding flaky yellow-orange crystals of **3** (141 mg, 63%). ^1H NMR (200 MHz, C_6D_6): δ 3.48 (broad s, 2H, CH_2=), 6.86 (m, 9H, *Ph*), 6.96 (m, 9H, *Ph*), 7.45 (dt, J = 8.4, 1.1 Hz, 6H, *Ph*), 7.80 (m, 6H, *Ph*). $^{13}C\{^1H\}$ NMR (67.9 MHz, C_6D_6): δ 55.7 (dt, $J_{C\text{-}H}$ = 154 Hz, $J_{Rh\text{-}C}$ = 20.4 Hz, =CH_2), 127.2 (*Ph*), 128.4 (*Ph*), 128.8 (P*Ph*), 129.1 (P*Ph*), 129.6 (P*Ph*), 130.0 (P*Ph*), 134.2 (d, $J_{P\text{-}C}$ = 12 Hz, P*Ph*), 134.7 (d, $J_{P\text{-}C}$ = 13 Hz, P*Ph*), 135.6 (d, $J_{P\text{-}C}$ = 37.9 Hz, P*Ph*), 137.6 (*Ph*), 138.3 (d, $J_{P\text{-}C}$ = 43.5 Hz, P*Ph*), 141.3 (*Ph*), 154.7 (d, $J_{Rh\text{-}C}$ = 4.6 Hz, =*C*(*O*)).

(24) Nixon, J. F.; Wilkins, B.; Clement, D. A. *J. Chem. Soc., Dalton Trans.* **1974**, 1993.
(25) Bottrill, M.; Green, M. *J. Organomet. Chem.* **1976**, *111*, C6.
(26) Volger, H. C.; Vrieze, K. *J. Organomet. Chem.* **1968**, *13*, 479.
(27) Clement, D. A.; Nixon, J. F.; Poland, J. S. *J. Organomet. Chem.* **1974**, *76*, 117.
(28) Brown, C. K.; Mowat, W.; Yagupsky, G.; Wilkinson, G. *J. Chem. Soc. A* **1971**, 850.
(29) Obtained from the reaction of pivalic acid and excess ethyllithium followed by a TMSCl quench and aqueous hydrolysis: Jorgenson, M. J. *Org. React.* **1971**, *18*, 1.
(30) Osborn, J. A.; Wilkinson, G. *Inorg. Synth.* **1967**, *10*, 67.
(31) Chatt, J.; Venanzi, L. M. *J. Chem. Soc. A* **1957**, 195.

Table 3. Crystal Structure Data for 6

empirical formula	$C_{48}H_{47}OP_2Rh$
color habit	orange block
cryst size (mm)	0.4 × 0.3 × 0.2
cryst syst	monoclinic
space group	$P2_1/c$
unit cell dimens	
a (Å)	9.762(3)
b (Å)	22.494(4)
c (Å)	18.077(4)
β (deg)	97.31(2)
volume (Å^3)	3937.3(15)
no. of peaks to determine cell	41
2θ range of cell peaks (deg)	19.0–54.0
Z	4
fw	804.7
density (calc) (Mg/m^3)	1.358
abs coeff (mm^{-1})	4.621
F(000)	1672
$R(F)$ (%)	5.13
$R_w(F)$ (%)	6.05

$^{31}P\{^1H\}$ NMR (109.4 Hz, C_6D_6): δ 38.8 (dd, J_{Rh-P} = 196.4 Hz, J_{P-P} = 35.5 Hz), 53.9 (dd, J_{Rh-P} = 225.6 Hz, J_{P-P} = 35.5 Hz). Three samples were submitted for analysis, and a wide range of analytical data was obtained. Analytical reports noted decomposition prior to combustion. Anal. Calcd for $C_{44}H_{37}OP_2Rh$: C, 70.79; H, 5.96. Found: C, 58.62 ± 1.84; H, 3.86 ± 0.08.

Preparation of (η^3-3,3-Dimethyl-2-oxobutenyl)bis(triphenylphosphine)rhodium (6). The procedure used in the preparation of **3** was followed, except potassium 3,3-dimethyl-2-oxidobutene (18 mg, 0.13 mmol) was added to the suspension of **1** (85 mg, 0.06 mmol). An orange-yellow powdery complex (52 mg, 56% yield) was isolated after recrystallization from hexane (~5 mL) at −60 °C. ^1H NMR (C_6D_6, 200 MHz): δ 1.24 (s, 9H), 2.82 (very broad s, 1H), 3.57 (very broad s, 1H), 7.90 (m, 18H), 7.75 (m, 12H). $^{13}C\{^1H\}$ NMR (C_6D_6, 125.8 MHz): δ 28.8 (q, J = 132 Hz, $(CH_3)_3C$), 38.4 (s, $(CH_3)_3C$), 54.3 (dd, J_{C-H} = 153 Hz, J_{Rh-C} = 23.5 Hz, $=CH_2$), 127.5 (d, J = 9.6 Hz, *Ph*), 127.8 (s, *Ph*), 128.3 (s, *Ph*), 128.9 (d, J = 18.1 Hz, *PPh*), 134.4 (d, J = 12.1 Hz, *PPh*), 134.7 (d, J = 12.8 Hz, *PPh*), 137.2 (d, J = 36.1 Hz, *Ph*), 138.9 (d, J = 42.0 Hz, *Ph*), 175.0 (d, J_{Rh-C} = 4.6 Hz, $=C(O)$). $^{31}P\{^1H\}$NMR (121.5 MHz, C_6D_6, internal 85% H_3PO_4 standard): δ 38.1 (dd, J = 193.0, 36.9 Hz), 55.7 (dd, J = 222.8, 36.9 Hz). IR (C_6H_6): 1440 (s), 1099 (s), 758 (broad m) cm^{-1}. Anal. Calcd for $C_{42}H_{41}OP_2Rh$: C, 69.46; H, 5.69. Found: C, 69.86; H, 5.72.

X-ray Crystal Structure of 6. X-ray quality crystals of **6** were grown from a saturated solution of C_6D_6 at room temperature. The structure of **6** was solved by direct methods on a Siemens P4 diffractometer (Table 3). All non-hydrogen atoms were refined independently with anisotropic thermal parameters by a full-matrix least-squares refinement method using SHELXTL PLUS/1989.[32]

Preparation of (η^3-1-Phenyl-1-oxoethenyl)bis(triethylphosphine)rhodium (8). In a glovebox, solid $[(COD)RhCl]_2$ (**7**; 250 mg, 0.51 mmol) was suspended in THF (10 mL), and a solution of PEt_3 (238 mg, 2.3 mmol) in THF (2 mL) was added dropwise over 6 min. After complete addition the orange-brown solution was stirred at 24 °C for 20 min. Solid potassium 1-phenyl-1-oxidoethene (**2**; 160 mg, 1.1 mmol) was added. On a vacuum line, the orange suspension was stirred vigorously for 42 min at 24 °C. The mixture was concentrated to a red oil, and pentane (~12 mL) was vacuum-distilled onto the residue. Insoluble salts were filtered on a reversible frit, and the solid was rinsed with pentane. The deep red-orange solution was concentrated to ~3 mL and cooled to −60 °C for 20 h. Red-orange crystals (323 mg, 70%) were isolated by cold filtration. ^1H NMR (200 MHz, C_6D_6): δ 0.80 (dt, J = 15.3, 7.7, 9H, CH_3), 1.07 (dt, J = 15.4, 7.7, 9H, CH_3), 1.26 (pentet, J = 7.5 Hz, 6H, P—CH_2), 1.55 (pentet, J = 7.5, 6H, P—CH_2), 3.27 (d, J = 4.9 Hz, 1H, anti-CH_2), 3.65 (d, J = 1.0 Hz, 1H, syn-CH_2), 7.18 (m, 3H), 8.04 (m, 2H). $^{13}C\{^1H\}$NMR (67.9 MHz, C_6D_6): δ 8.8 (PCH_2CH_3), 8.9 (PCH_2CH_3), 19.7 (d, J_{P-C} = 22.2 Hz, PCH_2CH_3), 21.7 (d, J_{P-C} = 27.7 Hz, PCH_2CH_3), 48.2 (dd, J_{C-H} = 154 Hz, J_{Rh-C} = 24.4 Hz, J_{P-C} = 4.4 Hz, $=CH_2$), 126.5 (*Ph*), 128.1 (*Ph*), 128.8 (*Ph*), 143.0 (*Ph*), 151.9 (d, J_{Rh-C} = 2.8 Hz, $=C(O)$). $^{31}P\{^1H\}$NMR (109.4 MHz, C_6D_6): δ 26.4 (dd, J = 188.4, 40.0 Hz), 43.0 (dd, J = 212.3, 40.0 Hz). IR (C_6H_6): 2964 (m), 2938 (m), 2880 (m), 1460 (m), 1344 (m), 758 (s) cm^{-1}. Anal. Calcd for $C_{20}H_{37}OP_2Rh$: C, 52.41; H, 8.08. Found: C, 52.11; H, 8.31.

Preparation of (η^3-(Z)-4,4-Dimethyl-3-oxo-2-pentenyl)bis(triethylphosphine)rhodium (10). The procedure used in the preparation of **7** was followed, except solid potassium (*Z*)-4,4-dimethyl-3-oxido-2-pentene (**9**; 167.2 mg, 1.1 mmol) was added to a solution of **7** (250 mg, 0.51 mmol) and PEt_3 (238 mg, 2.3 mmol) in THF (10 mL). After filtration of the insoluble KCl and concentration of the pentane solution, an orange oil remained. In a glovebox, the oil was dissolved in pentane (~2 mL) and cooled to −40 °C to facilitate recrystallization. After 72 h, gold-yellow plates (154 mg, 31%) were isolated by cold filtration. ^1H NMR (250 MHz, toluene-d_8): δ 0.97 (m, 18H, PCH_2CH_3), 1.30 (s, 9H, $C(CH_3)_3$), 1.47 (m, 12H, PCH_2CH_3), 1.62 (d, 3H, J = 6.0 Hz, $=CHCH_3$), 3.64 (dq, J = 6.0 Hz, J_{P-H} = 3.0 Hz, 1H, C(O)=*CH*). $^{13}C\{^1H\}$ NMR (100.6 MHz, C_6D_6): δ 8.6 (d, J_{P-C} = 12.6 Hz, PCH_2CH_3)), 8.9 (d, J_{P-C} = 28.9 Hz, PCH_2CH_3)), 19.4 (d, J_{P-C} = 19.5 Hz, PCH_2CH_3), 21.2 (d, J_{P-C} = 24.4 Hz, PCH_2CH_3), 28.6 ($C(CH_3)_3$), 38.4 ($C(CH_3)_3$), 56.4 (d, J_{Rh-C} = 23.9 Hz, $=CH$), 161.4 (d, J_{Rh-C} = 4.0 Hz, $=CO$). $^{31}P\{^1H\}$NMR (121.5 MHz, C_6D6): δ 25.3 (dd, J = 37 Hz, 179 Hz), 38.1 (dd, J = 37 Hz, 220 Hz). IR (C_5H_{12}): 1425 (m), 1344 (m), 1038 (s), 768 (s), 725 (s) cm^{-1}. Anal. Calcd for $C_{19}H_{43}OP_2Rh$: C, 50.44, H, 9.53. Found: C, 50.73; H, 9.54.

General Procedure for the Carbonylation of Rhodium Oxaallyl Complexes. Preparation of 11 and 12. A solution of $(Ph_3P)_2Rh(OC(Ph)=CH_2)$ (**3**; 10 mg, 0.013 mmol) in C_6D_6 (~0.3 mL) was added to a thick-wall NMR tube. The tube was fitted with a Cajon adapter which was attached to a three-way valve. In a fume hood, the valve was purged with CO for 5 min. Then the valve was opened to the tube, and CO was bubbled through the solution for 2 min. On a vacuum line the solution was degassed three times by freeze–pump–thaw cycles under high vacuum, and the tube was sealed.

Data for **11**: ^1H NMR (200 MHz, C_6D_6) δ 4.38 (broad s, 2H, $=CH_2$), 7.01 (broad s, 21H, P—*Ph* and *Ph*), 7.82 (broad s, 14H, P—*Ph* and *Ph*); IR (C_6H_6) 1965 (vs, Rh—CO) cm^{-1}. The NMR of **11** showed a signal at δ 2.08 (s) (9%) corresponding to acetophenone.

Data for **12**: ^1H NMR (200 MHz, C_6D_6) δ 1.03 (pentet, J = 7.7 Hz, 18H, PCH_2CH_3), 1.63 (m, 12H, PCH_2CH_3), 4.45 (s, 1H, C(O)=C*H*H), 4.70 (s, 1H, C(O)=CH*H*), 7.12 (m, 2H, *Ph*), 7.31 (t, J = 6.7 Hz, 1H, *Ph*), 8.09 (d, J = 7.2 Hz, 2H, *Ph*); IR (C_6H_6) 1945 (vs, Rh-CO) cm^{-1}. The NMR

(32) SHELXTL PLUS/1989, Siemens Analytical X-ray Instruments, Inc., Madison, WI 53719.

showed a signal at δ 2.08 (s) (8%) corresponding to acetophenone.

Preparation of *trans*-$(Et_3P)_2$(*t*-BuNC)Rh-(OC(Ph)=CH_2) (13). A solution of $(Et_3P)_2$Rh(OC-(Ph)=CH_2) (8; 9 mg, 0.020 mmol) in C_6D_6 (~0.3 mL) was prepared in a thick-walled NMR tube, and *t*-BuNC (2.4 μL, 0.020 mmol) was syringed into the tube. After mixing for 36 min, excess isocyanide and C_6D_6 were evaporated under vacuum. The yellow residue was dissolved in C_6D_6 (~0.3 mL), and the tube was sealed. ^{1}H NMR (200 MHz, C_6D_6): δ 1.04 (s, 9 H, C(CH_3)$_3$), 1.16 (broad s 18H, PCH_2CH_3), 1.69 (broad s, 12H, PCH_2CH_3), 4.70 (broad s, 2H, C(O)=CH_2), 7.16 (t, J = 5.6 Hz, 1H, *p*-*Ph*), 7.30 (t, J = 7.0 Hz, 2H, *o*-*Ph*), 8.24 (m, 2H, *m*-*Ph*). ^{13}C{^{1}H} NMR (69.9 MHz, C_6D_6): δ 8.9 (PCH_2CH_3), 17.1 (t, J_{P-C} = 10.6 Hz, PCH_2CH_3), 30.9 (C(CH_3)$_3$), 54.9 (*C*(CH_3)$_3$), 77.5 (OC-(Ph)=CH_2), 126.2 (*Ph*), 126.3 (t, J = 10.2 Hz, *t*-Bu*N*C), 126.5 (*Ph*), 128.5 (*Ph*), 144.2 (*Ph*), 167.6 (O*C*(Ph)=CH_2). ^{31}P{^{1}H} NMR (109.4 MHz, C_6D_6): δ 23.7 (d, J = 138.0 Hz). IR (C_6H_6): 2040 (vs), 1586 (m), 1561 (m) cm^{-1}. HRMS: calcd for $C_{25}H_{46}NOP_2Rh$ 541.2109, found 541.2078 (0.11% of base peak).

Preparation of $(Ph_3P)_2$(*t*-BuNC)$_2$Rh-CH_2C(O)*t*-Bu (16). Solid $(Ph_3P)_2$Rh(OC(*t*-Bu)=CH_2) (6; 12 mg, 0.016 mmol) was dissolved in C_6D_6 (0.3 mL), and *t*-BuNC (2.7 mg, 0.033 mmol, 29.0 mL volume bulb at 2 mmHg) was layered onto the solution by vacuum transfer techniques. The mixture was agitated at room temperature for 20 min, and a bright yellow solution of **16** resulted. The solution was degassed twice by the freeze–pump–thaw method, and the NMR tube was sealed. ^{1}H NMR (200 MHz, C_6D_6): δ 0.90 (s, 18 H, CNC(CH_3)$_3$), 1.75 (s, 9H, C(CH_3)$_3$), 3.34 (d, J_{Rh-H} = 3.3 Hz, 2H, Rh-CH_2C(O)), 7.06 (broad s, 18H, P—*Ph*), 7.63 (broad s, 12H, P—*Ph*); ^{13}C{^{1}H} NMR (69.9 MHz, C_6D_6): 30.0 (CNC(CH_3)$_3$), 30.1 (C(CH_3)$_3$), 33.4 (CN*C*(CH_3)$_3$), 42.0 (*C*(CH_3)$_3$), 55.4 (d, J_{Rh-C} = 12 Hz, Rh—CH_2 C(O), 128.5 (*Ph*), 128.36 (*Ph*), 134.35 (dd, J = 11, 83 Hz, *t*-Bu*N*C), 134.6 (*Ph*), 138.3 (*Ph*), 217.5 (*C*(O)). IR (C_6H_{14}): 2110 (vs), 2074 (w) (intensity dependent upon sample purity), 1613 (m) cm^{-1}.

Acknowledgment. We gratefully acknowledge the generous support of the National Science Foundation (Grant No. CHE-9200699). J.R.A. thanks the Howard Hughes Medical Foundation for a summer research assistantship. We also acknowledge Johnson Matthey for a generous loan of $RhCl_3 \cdot H_2O$.

Supplementary Material Available: Figures giving ^{1}H NMR and ^{13}C NMR spectra for **3**, **6**, **8**, and **10** and tables of structure determination data, positional and anisotropic thermal parameters for non-hydrogen atoms, selected interatomic distances and angles, and idealized atomic parameters for hydrogen atoms for **6** (15 pages). Ordering information is given on any current masthead page.

OM930596H